10.1098/rsta.2001.0933

THE ROYAL SOCIETY

Towards the simplest hydrodynamic lattice-gas model

By Bruce M. Boghosian[1], Peter J. Love[2] and David A. Meyer[3]

[1]*Department of Mathematics, Tufts University, Bromfield-Pearson Hall, Medford, MA 02155, USA* (bruce.boghosian@tufts.edu)

[2]*Centre for Computational Science, Queen Mary, University of London, Mile End Road, London E1 4NS, UK* (p.j.love@qmw.ac.uk)

[3]*Department of Mathematics, University of California, San Diego, La Jolla, CA 92093-0112, USA* (dmeyer@math.ucsd.edu)

Published online 12 February 2002

It has been known since 1986 that it is possible to construct simple lattice-gas cellular automata whose hydrodynamics are governed by the Navier–Stokes equations in two dimensions. The simplest such model heretofore known has six bits of state per site on a triangular lattice. In this work, we demonstrate that it is possible to construct a model with only five bits of state per site on a Kagome lattice. Moreover, the model has a simple, deterministic set of collision rules and is easily implemented on a computer. In this work, we derive the equilibrium distribution function for this lattice-gas automaton and carry out the Chapman–Enskog analysis to determine the form of the Navier–Stokes equations.

Keywords: lattice-gas automata; hydrodynamics; Navier–Stokes equations; Kagome lattice

1. Introduction

Hydrodynamic lattice-gas automata are idealized microscopic models of fluids, designed so that their bulk behaviour is governed by the Navier–Stokes equations. The models consist of fictitious 'molecules,' constrained to move along the edges of a lattice, which interact by collisions that conserve mass, momentum and energy.

The earliest model along these lines was devised and studied by Kadanoff & Swift (1968) (referred to below as the KS model). They considered a two-dimensional Cartesian lattice, each site of which may be occupied by a single particle. Each particle is tagged by a momentum vector, oriented along one of the four diagonals of the Cartesian lattice. Dynamics are then defined which conserve mass, momentum and energy, and obey the principle of detailed balance. The KS model exhibits many features of real fluids, as the authors noted, however, its bulk behaviour is not governed by the Navier–Stokes equations. In particular, the dynamics are anisotropic: dependent on the orientation of the underlying lattice.

The next advance in the lattice modelling of fluids came in the mid 1970s, when Hardy, de Pazzis & Pomeau (HPP) introduced a new lattice model with a number of interesting innovations (Hardy *et al*. 1973, 1976). The HPP model also resides on a two-dimensional Cartesian lattice. Particles move along the edges of the Cartesian

lattice and there may not be more than one particle with a particular velocity, at a particular site, at a particular time. This 'exclusion principle' makes it possible to represent the state of any site $\boldsymbol{x}$ by four bits of information; bit $n_j(\boldsymbol{x}, t)$, where $j \in \{1, 2, 3, 4\}$, encodes the presence (1) or absence (0) of a particle with velocity $\boldsymbol{c}_j$ at site $\boldsymbol{x}$ and time t. At each time-step, particles at each site experience a purely local *collision*, which conserves mass and momentum. After the collisions, all particles 'stream' to the site in the direction of their velocity vector.

Like the KS model, the HPP model gives rise to anisotropic hydrodynamic equations. The HPP model suffers from a number of other defects; in particular, if it is implemented on a rectangular lattice with periodic boundary conditions, the total number of particles moving along each row and each column is conserved. If the lattice has even dimensions in the x- and y-directions, so that it may be painted as a checkerboard, the total numbers of particles on white and black squares are conserved separately. These unphysical *spurious invariants* have no analogue in a continuum fluid, and are therefore an undesirable feature of the model.

The anisotropy problem was solved by Frisch *et al.* (1986), and roughly simultaneously by Wolfram (1986). The FHP lattice gas, named after the authors of the first reference given above (Frisch, Hasslacher and Pomeau), is very similar to that of HPP in that the particles are associated with the lattice vectors, and the evolution proceeds by alternating collision and streaming steps. The principal difference is that it is implemented on a triangular lattice instead of a Cartesian one. Now one would expect that a sixfold symmetric lattice would give rise to a more isotropic model than a fourfold symmetric one. The surprising result of the 1986 studies, however, is that the sixfold version does not only improve the isotropy, it yields *perfect* isotropy. The reason for this has to do with the invariance properties of fourth-rank tensors: the only fourth-rank tensors that are invariant under 60° rotation are isotropic, whereas there exist anisotropic fourth-rank tensors that are invariant under 90° rotation. In particular, if we denote the lattice vectors by $\boldsymbol{c}_i$, where $0 \leqslant i < b$, the sum of their fourfold outer product,

$$\sum_{i=0}^{b-1} \boldsymbol{c}_i \boldsymbol{c}_i \boldsymbol{c}_i \boldsymbol{c}_i,$$

is isotropic for the triangular lattice ($b = 6$), but anisotropic for the Cartesian lattice ($b = 4$).

The FHP collisions that conserve mass and momentum are illustrated in figure 1. Note that the two-body collision is non-deterministic; the outcome must be decided by a stochastic process. The three-body collision is necessary to prevent the existence of a spurious invariant; without it, momentum would be separately conserved along each of the three lattice directions, rather than just along two orthogonal directions as is appropriate for a two-dimensional fluid. The model may also be extended to include (non-deterministic) four-body collisions which are identical to the two-body collisions if one simply replaces particles by holes.

The result of this 1986 work was a lattice gas whose coarse-grained behaviour was that of a Navier–Stokes fluid. The actual equations of motion possess certain anomalies, such as a factor in front of the inertial term that breaks Galilean invariance, and a pressure that depends on the hydrodynamic velocity, but these problems are inconsequential as long as one uses the model to simulate an *incompressible* viscous fluid. These anomalies will be revisited below in the context of the new model pre-

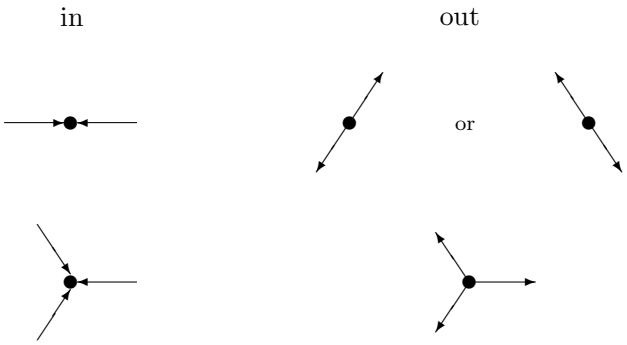

Figure 1. Non-trivial collisions of the FHP lattice gas. The dynamics takes place on a triangular lattice in two dimensions. The symmetric three-body collision is necessary to avoid a third spuriously conserved component of momentum. Asymmetric three-body and four-body collisions are also possible, but are not illustrated here.

sented in this paper. The interested reader may also consult the texts by Rothman & Zaleski (1997) and by Rivet & Boon (2001) for more information about the early development of lattice-gas models.

2. The Kagome lattice

It is interesting to note that triangular lattices have also been used to study *frustration* in two-dimensional Ising antiferromagnets (Syôzi 1951). The Hamiltonian for an Ising antiferromagnet has lower energy when neighbouring spins have opposite direction. On a Cartesian lattice, there is a ground state in which the lattice is coloured like a checkerboard and spins on white squares point up/down, while those on black squares point down/up; note that this ground state has degeneracy of only two. On a triangular lattice, by contrast, any two neighbouring spins have two more common neighbours. If the given neighbouring spins are oppositely oriented, their common neighbours have no preferred orientation, leading to ground states with huge degeneracy. Such 'geometric frustration' is interesting and the subject of much current research.

Remarkably, the spin-$\frac{1}{2}$ Heisenberg antiferromagnet on a triangular lattice does exhibit long-range order in spite of the above-described geometric frustration. This is thought to be related to the triangular lattice's high coordination number of 6. For this reason, researchers have turned their attention to spin models on the Kagome lattice, illustrated in figure 2. Like the Cartesian lattice, the Kagome lattice has coordination number 4. Like the triangular lattice, it is capable of exhibiting geometric frustration, since some of the plaquettes are triangles. Unlike either the Cartesian or triangular lattices, however, a spin-$\frac{1}{2}$ Heisenberg antiferromagnet on the Kagome lattice does not seem to exhibit any long-range order. It is therefore the subject of some intense scrutiny.

3. Kagome hydrodynamic lattice gas

The principal observation of this paper is that the Kagome lattice is also very well suited to the construction of a hydrodynamic lattice-gas model. Lattice vectors align

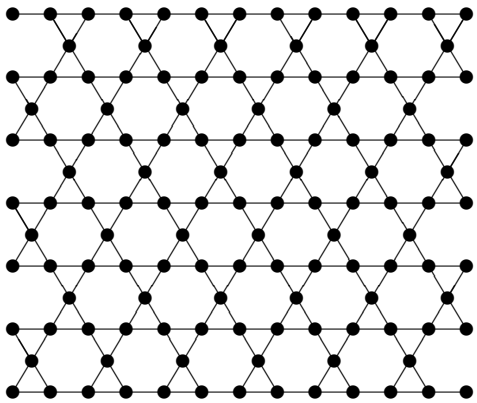

Figure 2. Kagome lattice.

so that particles are free to move in straight lines if they do not collide. The lattice has sixfold symmetry, so the emergent hydrodynamics are isotropic. Finally, each site of the model has only four lattice vectors, paired in opposite directions. This suggests that the HPP rules could be resurrected and used on this lattice, but that would lead to the problem of momentum being conserved separately along three directions; this is the same problem mentioned above in the context of the FHP lattice gas, which was solved by the addition of the three-body collisions. On the Kagome lattice, we solve this problem instead by allowing for a rest particle of mass two. Two particles arriving from opposite directions at a site with no rest particle may then 'stick' to form a mass-two rest particle; two particles arriving from opposite directions at a site with a rest particle already present may then 'free' this particle, releasing two moving particles in the other unoccupied directions. Note that this collision process is perfectly deterministic; there is no stochastic aspect to it, as there is with the two-body collisions in the FHP lattice gas. The result is a perfectly isotropic hydrodynamic lattice gas with only five bits per site.

Each site of the hydrodynamic lattice-gas model on the Kagome lattice may be represented by five bits of state. The first four represent the moving particles of mass one listed in counterclockwise order, and the fifth represents the rest particle of mass two. Each site may thus be in one of $2^5 = 32$ possible states. These states may be enumerated by regarding the five bits as the binary representation of a number, from least-significant bit to most-significant bit. The precollision and postcollision states at a site may each be represented by a number from 0 to 31; given the former, the collision rule determines the latter. Thus, the collision process may be viewed as a map from the set $\{0, \ldots, 31\}$ onto itself. This map, based on the rule described at the end of the last section, is given in table 1.

A problem with the representation described above is that the lattice vectors are different from site to site. For this reason, it is easier to analyse the model by grouping triplets of sites, as shown in figure 3. Each circle in this figure encloses a group of three sites. We note that these groups are arranged on an ordinary triangular lattice. Hence, in the spirit of spatial block renormalization, we may regard each group as being a single site that may be represented by 15 bits of state. It is manifest that this 'blocked' lattice-gas model with 15 bits per site has the same hydrodynamic limit as the original model. At the end of the calculation, it will be necessary to understand

Table 1. *Collision rule for the Kagome lattice-gas model.*

in	out	in	out	in	out	in	out
0	0	8	8	16	16	24	13
1	1	9	9	17	11	25	25
2	2	10	5	18	7	26	21
3	3	11	17	19	19	27	27
4	4	12	12	20	14	28	28
5	10	13	24	21	26	29	29
6	6	14	20	22	22	30	30
7	18	15	15	23	23	31	31

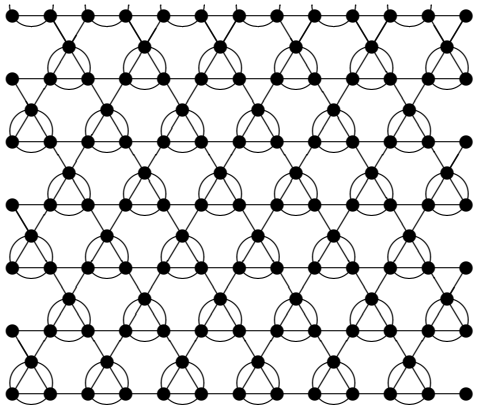

Figure 3. Grouping of sites.

that the blocked lattice spacing is 2ℓ, where ℓ is the original spacing on the Kagome lattice.

In figure 4, we label the 15 lattice vectors associated with a single group of three sites. Note that the directions labelled 0 through 5 and the directions labelled 6 through 11 are the six lattice vectors on a triangular lattice, counting in the counter-clockwise direction. Directions 12 through 14 are then reserved for the rest particles.

We may define the mass associated with the particle in direction j,

$$m_j = \begin{cases} 1 & \text{if } 0 \leqslant j < 12 \text{ (moving)}, \\ 2 & \text{if } 12 \leqslant j < 15 \text{ (rest)}, \end{cases} \tag{3.1}$$

and the momentum associated with the particle in direction j,

$$\boldsymbol{p}_j = \begin{cases} \hat{\boldsymbol{x}} \cos(\frac{2}{6}\pi j) + \hat{\boldsymbol{y}} \sin(\frac{2}{6}\pi j) & \text{if } 0 \leqslant j < 12 \text{ (moving)}, \\ \boldsymbol{0} & \text{if } 12 \leqslant j < 15 \text{ (rest)}. \end{cases} \tag{3.2}$$

During the streaming step, particles 0 through 5 will move to a neighbouring site. Note that particles 6 through 11 do not stream on the 'blocked' lattice, in spite of the fact that they have momentum and did stream on the original lattice. On the blocked lattice, particle j at site $\boldsymbol{x}$ streams to become particle $\sigma(j)$ at site $\boldsymbol{x} + \boldsymbol{c}_j$,

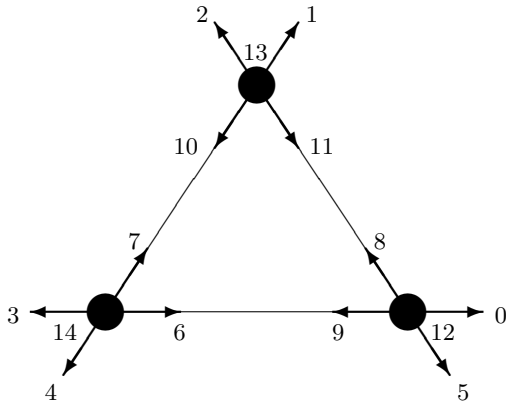

Figure 4. Labelling for one group of sites.

where

$$\boldsymbol{c}_j = 2\begin{cases}\hat{\boldsymbol{x}}\cos(\frac{2}{6}\pi j) + \hat{\boldsymbol{y}}\sin(\frac{2}{6}\pi j) & \text{if } 0 \leqslant j < 6,\\ \boldsymbol{0} & \text{if } 6 \leqslant j < 15,\end{cases} \tag{3.3}$$

and

$$\sigma(j) = \begin{cases} j+6 & \text{for } 0 \leqslant j < 6,\\ j-6 & \text{for } 6 \leqslant j < 12,\\ j & \text{for } 12 \leqslant j < 15.\end{cases} \tag{3.4}$$

We note that $\boldsymbol{p}_j \neq m_j \boldsymbol{c}_j$!

It may be verified that

$$\sum_{j=0}^{14} \boldsymbol{p}_j \boldsymbol{p}_j = 6\boldsymbol{\Omega}_{(2)}, \tag{3.5}$$

$$\sum_{j=0}^{14} \boldsymbol{p}_j \boldsymbol{p}_j \boldsymbol{p}_j \boldsymbol{p}_j = \tfrac{3}{2}\boldsymbol{\Omega}_{(4)}, \tag{3.6}$$

where we have defined the completely symmetric and isotropic tensors of second and fourth rank:

$$\boldsymbol{\Omega}_{(2)_{\alpha\beta}} = \delta_{\alpha\beta}, \tag{3.7}$$

$$\boldsymbol{\Omega}_{(4)_{\alpha\beta\mu\nu}} = \delta_{\alpha\beta}\delta_{\mu\nu} + \delta_{\alpha\mu}\delta_{\beta\nu} + \delta_{\alpha\nu}\delta_{\beta\mu}. \tag{3.8}$$

Similar sums of odd-rank outer products of the lattice vectors vanish. The rank-four condition above guarantees isotropy of the resultant hydrodynamic model.

4. Kinetic equations

The microscopic kinetic equation for the Kagome lattice gas is

$$n_{\sigma(j)}(\boldsymbol{x} + \boldsymbol{c}_j, t + \Delta t) = n_j(\boldsymbol{x}, t) + \Omega_j[n_*(\boldsymbol{x}, t)], \tag{4.1}$$

where Ω_j denotes the collision operator, defined at a 'blocked' site, with 15 bits of state. We imagine that we have an entire ensemble of such lattice gases, differing only in their initial conditions, and we define the ensemble average

$$N_j(\boldsymbol{x}, t) \equiv \langle n_j(\boldsymbol{x}, t) \rangle. \tag{4.2}$$

We take the ensemble average of the microscopic kinetic equation, ignoring correlations between the 15 bit-valued arguments of the collision operator. That is, we ignore correlations between particles entering a collision; this is Boltzmann's 'molecular chaos assumption'. With this assumption in place, the average of the collision operator is equal to the collision operator of the averages, and we may write

$$N_{\sigma(j)}(\boldsymbol{x} + \boldsymbol{c}_j, t + \Delta t) = N_j(\boldsymbol{x}, t) + \Omega_j[N_*(\boldsymbol{x}, t)]. \tag{4.3}$$

This is the lattice Boltzmann equation for the Kagome lattice gas.

If the collision operator were not present, the lattice Boltzmann equation would describe only the streaming of the particle j along the vector $\boldsymbol{c}_j$. The collision operator is designed to describe the collisions by depleting the directions of particles entering a collision, and augmenting the directions of particles exiting a collision. Each 'blocked' site of the lattice gas has 15 bits of state, and hence 2^{15} possible states. We let s be an index that ranges over all these states; for example, s may be an integer that takes on values from 0 to $2^{15} - 1$. We denote by $C(s)$ the postcollision state that results from precollision state s. We denote by s_j and $C_j(s)$ the value of the jth bit of states s and $C(s)$, respectively. With this notation established, the collision operator is given by

$$\Omega_j[n_*] = \sum_s p_s(n_*)[C_j(s) - s_j], \tag{4.4}$$

where $p_s(n_*)$ is equal to one if the bits n_* are in state s and zero otherwise. That is, we may write

$$p_s(n_*) = \prod_k n_k^{s_k}(1 - n_k)^{1 - s_k}. \tag{4.5}$$

The ensemble-averaged collision operator in the Boltzmann approximation is then

$$\Omega_j[N_*] = \sum_s p_s(N_*)[C_j(s) - s_j]. \tag{4.6}$$

5. Local thermodynamic equilibrium

As is well known (Frisch *et al.* 1987), setting the collision operator equal to zero results in the Fermi–Dirac equilibrium distribution

$$N_j^{\mathrm{lte}} = \frac{1}{1 + \exp(-\mu m_j - \boldsymbol{\gamma} \cdot \boldsymbol{p}_j)}, \tag{5.1}$$

where the quantities μ and $\boldsymbol{\gamma}$ are determined by the conserved quantities

$$\rho = \sum_{j=0}^{14} N_j^{\mathrm{lte}} m_j, \tag{5.2}$$

$$\boldsymbol{\pi} = \sum_{j=0}^{14} N_j^{\mathrm{lte}} \boldsymbol{p}_j. \tag{5.3}$$

We expand this in Mach number to obtain

$$N_j^{\mathrm{lte}} = \begin{cases} \dfrac{\mathrm{e}^{\mu}}{1+\mathrm{e}^{\mu}} - \dfrac{\mathrm{e}^{\mu}}{(1+\mathrm{e}^{\mu})^2}\boldsymbol{\gamma}\cdot\boldsymbol{p}_j + \dfrac{\mathrm{e}^{\mu}(1-\mathrm{e}^{\mu})}{2(1+\mathrm{e}^{\mu})^3}\boldsymbol{\gamma}\boldsymbol{\gamma}:\boldsymbol{p}_j\boldsymbol{p}_j + \mathcal{O}(|\boldsymbol{\gamma}|^3) & \\ \qquad\qquad\qquad\qquad\qquad\qquad\qquad\qquad\qquad\qquad \text{if } 0 \leqslant j \leqslant 11 \text{ (moving)}, \\ \dfrac{\mathrm{e}^{2\mu}}{1+\mathrm{e}^{2\mu}} \qquad\qquad\qquad\qquad\qquad\qquad\qquad\qquad\qquad\qquad \text{if } 12 \leqslant j \leqslant 14 \text{ (rest)}, \end{cases} \tag{5.4}$$

where the colon is used to denote a double inner product when this notation does not lead to ambiguity. We insert this into equation (5.3) and use equations (3.5) and (3.6) to obtain

$$\boldsymbol{\pi} = -6\left[\frac{\mathrm{e}^{\mu}}{(1+\mathrm{e}^{\mu})^2}\right]\boldsymbol{\gamma}. \tag{5.5}$$

We now use this to eliminate $\boldsymbol{\gamma}$ in favour of $\boldsymbol{\pi}$. Also, since the dependence on μ is unwieldy, we eliminate it in favour of the quantity

$$F \equiv \frac{\mathrm{e}^{\mu}}{1+\mathrm{e}^{\mu}},$$

by making the replacement

$$\mu = \ln\left(\frac{F}{1-F}\right).$$

We finally get

$$N_j^{\mathrm{lte}} = \begin{cases} F + \frac{1}{6}\boldsymbol{\pi}\cdot\boldsymbol{p}_j + \dfrac{1-2F}{72F(1-F)}\boldsymbol{\pi}\boldsymbol{\pi}:\boldsymbol{p}_j\boldsymbol{p}_j + \mathcal{O}(|\boldsymbol{\pi}|^3) & \text{if } 0 \leqslant j \leqslant 11 \text{ (moving)}, \\ \dfrac{F^2}{1-2F+2F^2} & \text{if } 12 \leqslant j \leqslant 14 \text{ (rest)}. \end{cases} \tag{5.6}$$

Next, we set about determining F (and thereby μ) in terms of the density ρ and the momentum density $\boldsymbol{\pi}$. Using equations (5.2) and (3.5), we get

$$\frac{\rho}{6} = \frac{F(2-3F+4F^2)}{1-2F+2F^2} + \frac{(1-2F)}{72F(1-F)}|\boldsymbol{\pi}|^2 + \mathcal{O}(|\boldsymbol{\pi}|^3). \tag{5.7}$$

This may be solved perturbatively, yielding

$$F = f - \frac{(1-2f)(1-2f+2f^2)^2}{144f(1-f)(1-3f+7f^2-8f^3+4f^4)}|\boldsymbol{\pi}|^2 + \mathcal{O}(|\boldsymbol{\pi}|^3), \tag{5.8}$$

where f is the solution to the zeroth-order equation

$$\frac{\rho}{6} = \frac{f(2-3f+4f^2)}{1-2f+2f^2}. \tag{5.9}$$

Inserting this solution for F into equations (5.6), and retaining terms to order $|\boldsymbol{\pi}|^2$, we finally get the Mach number expansion of the equilibrium distribution function

$$N_j^{\mathrm{lte}} = h_j(f) + \tfrac{1}{6}\boldsymbol{\pi}\cdot\boldsymbol{p}_j + \tfrac{1}{3}g(f)\boldsymbol{\pi}\boldsymbol{\pi}:[\boldsymbol{p}_j\boldsymbol{p}_j - \tfrac{1}{2}s_j(f)\mathbf{1}] + \mathcal{O}(|\boldsymbol{\pi}|^3), \tag{5.10}$$

where we have defined

$$g(f) \equiv \frac{1-2f}{24f(1-f)}, \tag{5.11}$$

$$h_j(f) \equiv \begin{cases} h_{\mathrm{M}}(f) \equiv f & \text{if } 0 \leqslant j \leqslant 11 \text{ (moving)}, \\ h_{\mathrm{R}}(f) \equiv \dfrac{f^2}{1-2f+2f^2} & \text{if } 12 \leqslant j \leqslant 14 \text{ (rest)}, \end{cases} \tag{5.12}$$

$$s_j(f) \equiv \begin{cases} s_{\mathrm{M}}(f) \equiv \dfrac{(1-2f+2f^2)^2}{1-3f+7f^2-8f^3+4f^4} & \text{if } 0 \leqslant j \leqslant 11 \text{ (moving)}, \\ s_{\mathrm{R}}(f) \equiv \dfrac{2f(1-f)}{1-3f+7f^2-8f^3+4f^4} & \text{if } 12 \leqslant j \leqslant 14 \text{ (rest)}, \end{cases} \tag{5.13}$$

where the subscripts 'M' and 'R' denote 'moving' and 'rest', respectively. Note that $N_j^{\mathrm{lte}} = N_{\sigma(j)}^{\mathrm{lte}}$. Equations (5.2) and (5.3) may then be verified using equations (3.5) and (3.6), and the easily verified identities

$$\rho = \sum_{j=0}^{14} m_j h_j(f) = 12h_{\mathrm{M}}(f) + 6h_{\mathrm{R}}(f), \tag{5.14}$$

$$12 = \sum_{j=0}^{14} m_j s_j(f) = 12s_{\mathrm{M}}(f) + 6s_{\mathrm{R}}(f). \tag{5.15}$$

6. Chapman–Enskog analysis

We have defined a remarkably simple lattice-gas model and demonstrated that it has a well-defined thermodynamic equilibrium. The Chapman–Enskog analysis may then be carried out to demonstrate that it obeys the Navier–Stokes equations in the thermodynamic limit. This is an asymptotic expansion in Knudsen number, Kn, which is the ratio of mean-free path to scale length. Since a mean-free path is of the order of the lattice spacing ℓ, terms of the form $\boldsymbol{c}_j \cdot \nabla \boldsymbol{u}$, for example, are first order in Knudsen number. As described in the last section, we also expand in Mach number M to obtain the incompressible limit. Indeed, we take $M \sim Kn$, so that the Reynolds number $Re \sim M/Kn$ is order unity in the scaling limit.†

The details of the Chapman–Enskog analysis are well described by Frisch *et al.* (1987) and by Hénon (1987), and we present only the results here. In the incompressible limit, the hydrodynamic velocity

$$\boldsymbol{u} = \boldsymbol{\pi}/\rho \tag{6.1}$$

and the pressure

$$P = 6f + \tfrac{1}{2}[1 - 2s_{\mathrm{M}}(f)]g(f)|\boldsymbol{\pi}|^2 \tag{6.2}$$

obey the equations

$$\nabla \cdot \boldsymbol{u} = 0, \tag{6.3}$$

$$\frac{\partial \boldsymbol{u}}{\partial t} + g(f)\boldsymbol{u} \cdot \nabla \boldsymbol{u} = -\frac{1}{\rho}\nabla P + \nu(f)\nabla^2 \boldsymbol{u}. \tag{6.4}$$

† This does not mean that the Reynolds number needs to be near unity; rather it means that the Reynolds number approaches a finite value—between zero and infinity—in the scaling limit.

Here $g(f)$ is given by equation (5.11) with f determined in terms of ρ by equation (5.9); also, the viscosity is given by

$$\nu(f) \equiv \frac{3 - 23f + 107f^2 - 340f^3 + 792f^4 - 1380f^5 \\ +1804f^6 - 1728f^7 + 1152f^8 - 480f^9 + 96f^{10}}{64f(1-f)(1-f+f^2)(1-3f+7f^2-8f^3+4f^4)^2} - \frac{1}{8}. \tag{6.5}$$

In all of the above, ρ and f should be regarded as constant; or, more precisely, their deviation from constancy is of order Kn^2.

The presence of the factor $g(f)$ in front of the inertial term is reflective of a breakdown in Galilean invariance. This is not surprising, since the lattice itself establishes a preferred Galilean frame. This anomaly is inconsequential in the incompressible limit, since it may be removed by simply scaling the hydrodynamic velocity; that is, the modified velocity $\boldsymbol{U} = g(f)\boldsymbol{u}$ obeys the Galilean-invariant Navier–Stokes equations. As noted above, in the incompressible limit, ρ is constant, hence f is constant, and hence the scaling factor $g(f)$ is also constant.

The equation of state, equation (6.2), indicates that the pressure depends on the hydrodynamic velocity. This seems anomalous, since it is not the case for real compressible fluids. Again, however, this anomaly is inconsequential as long as one adheres to the incompressible limit. In this limit, we may take divergence of both sides of equation (6.4), using equation (6.3) to obtain

$$\nabla^2 P = -\rho g(f) \nabla \cdot (\boldsymbol{u} \cdot \nabla \boldsymbol{u}), \tag{6.6}$$

indicating that the pressure is specified by a solution of the appropriate Poisson equation, rather than the equation of state, in this limit.

Finally, we note that the Reynolds number is given by the product of the lattice size, the Mach number, and the dimensionless function

$$R^*(\rho) = \frac{g(f)\rho(f)}{\nu(f)}. \tag{6.7}$$

A plot of R^* versus ρ is shown in figure 5. This indicates that, toward the goal of maximizing attainable Reynolds number, the optimal density is when $f \sim 0.3706$, and the corresponding value of R^* is 1.005 67.

7. Conclusions

We have demonstrated that a lattice-gas automaton with only five bits per site is sufficient to recover the Navier–Stokes equations in two dimensions. The model is defined on the Kagome lattice. Its deterministic collision rules are similar to those for the HPP gas with a rest particle. It yields isotropic hydrodynamic equations with anomalies similar to those of the FHP lattice gas. In the incompressible limit, these anomalies may be removed in the same way that they are for the FHP lattice gas, yielding a remarkably simple lattice-gas model for the Navier–Stokes equations.

The question naturally arises as to whether a simpler lattice gas may be constructed than that presented here. There are only two ways of making a simpler model: use a lattice of coordination number 4 which does not require rest particles, or a lattice of coordination number 3 which has one or no rest particles. Requiring

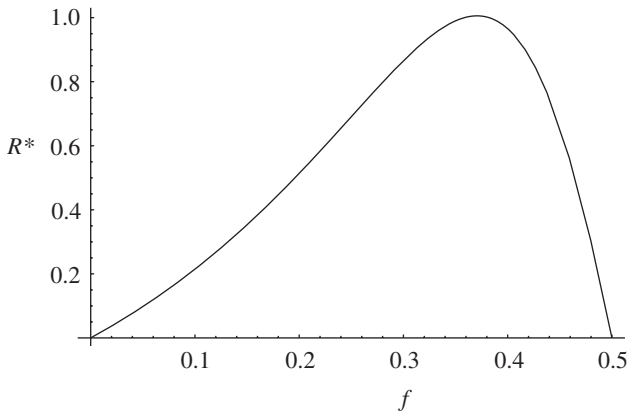

Figure 5. Value of R^* as a function of f.

that a coordination number 4 lattice must reproduce sixfold symmetry and satisfy the property that the lattice vectors sum to zero constitutes a definition of the Kagome lattice. Considering coordination number 3 one can obviously do the block renormalization on the edges of a tiling of hexagons, and regain the FHP lattice. The resulting three lattice vectors do not sum to zero, and so it is not possible to implement local deterministic collision rules which conserve momentum on this lattice. Non-local collision rules or rules which conserve momentum on average would require the storage of more than one bit per site.

It would be useful if the generalization introduced in this paper—allowing the set of lattice vectors to vary from site to site—could be extended to lattice-gas models in three spatial dimensions. There is a three-dimensional lattice, constructed by stacking tetrahedra, that is at least superficially analogous to the Kagome lattice. It is called the *pyrochlore* lattice and has coordination number 6. Though a six-bit model in three dimensions would indeed be a nice breakthrough, it turns out that the pyrochlore lattice lacks the symmetry requisite for isotropy. Thus, we leave to future work the question of extending this methodology to three spatial dimensions.

This work arose from informal discussions among the three authors at the NATO Advanced Research Workshop on 'Discrete Simulation of Fluid Dynamics: New Trends, New Perspectives', held in Cargèse, Corsica, from 2–7 July 2001. The authors therefore extend their thanks to the organizers of that meeting for providing an atmosphere that facilitated such discussion. In addition, B.M.B. and D.A.M. thank the Air Force Office of Scientific Research for support during the summer of 2001, when this work was conducted.

References

Frisch, U., Hasslacher, B. & Pomeau, Y. 1986 *Phys. Rev. Lett.* **56**, 1505.

Frisch, U., d'Humières, D., Hasslacher, B., Lallemand, P., Pomeau, Y. & Rivet, J.-P. 1987 Lattice-gas hydrodynamics in two and three dimensions. *Complex Syst.* **1**, 648.

Hénon, M. 1987 *Adv. Complex Syst.* **1**, 763.

Hardy, J., de Pazzis, O. & Pomeau, Y. 1973 *J. Math. Phys.* **14** 1746–1759.

Hardy, J., de Pazzis, O. & Pomeau, Y. 1976 *Phys. Rev.* **13**, 1949.

Kadanoff, L. P. & Swift, J. 1968 *Phys. Rev.* **165**, 310.

Rivet, J.-P. & Boon, J. P. 2001 *Lattice gas hydrodynamics*. Cambridge University Press.

Rothman, D. H. & Zaleski, S. 1997 *Lattice gas automata: simple models of complex hydrodynamics*. Cambridge University Press.

Syôzi, I. 1951 *Prog. Theor. Phys.* **6**, 306.

Wolfram, S. 1986 *J. Stat. Phys.* **45**, 471.